

**COVER SHEET**

*NOTE: This coversheet is intended for you to list your article title and author(s) name only  
—this page will not appear on the CD-ROM.*

Paper Number: **407**

**Title: Experimental methods to characterize the woven composite prepeg behavior during the preforming process**

Authors: Weizhao Zhang<sup>1</sup>

Huaqing Ren<sup>1</sup>

Jie Lu<sup>1</sup>

Zixuan Zhang<sup>1</sup>

Lingxuan Su<sup>2</sup>

Q Jane Wang<sup>1</sup>

Danielle Zeng<sup>2</sup>

Xuming Su<sup>2</sup>

Jian Cao<sup>1</sup>

## ABSTRACT

This paper reports several characterization methods of the properties of the uncured woven prepreg during the preforming process. The uniaxial tension, bias-extension, and bending tests are conducted to measure the in-plane properties of the material. The friction tests utilized to reveal the prepreg-prepreg and prepreg-forming tool interactions. All these tests are performed within the temperature range of the real manufacturing process. The results serve as the inputs to the numerical simulation for the product prediction and preforming process parameter optimization.

## INTRODUCTION

Woven carbon fiber composites have received increasing attention because of their high strength-to-weight ratio and excellent corrosion resistance [1]. Utilization of these composites in the transportation field can lead to weight reduction for fuel economy [2], making them attractive to industries. In recent decades, woven carbon fiber composites have been successfully used in the aerospace industry. However, because of the high demand for human labor to manually lay out the material, the cost is unacceptable for the parts used in high-volume vehicles.

To manufacture the woven carbon fiber composite parts in mass production, an automatic method is proposed: first, several layers of the uncured prepreg are stacked in proper orientations; then in the preforming process, these 2D planes are deformed into the rough shape of the 3D part via a press machine; finally, this 3D part is heated in a mold at a higher temperature to cure the epoxy in the material and fix the shape of the part. Compared to the traditional method, this new manufacturing process reduces the process cost by utilizing the preforming process with a press machine to replace the labor-consuming hand-lying work for the composite layers.

The preforming process is a derivation of the metal forming process. Currently, the parameter design for this process relies on trial-and-error with numerous tests and

---

<sup>1</sup>Northwestern University, 2145 Sheridan Road, Evanston, IL 60208, U.S.A.

<sup>2</sup>Ford Motor Company, Dearborn, MI 48124, U.S.A.

prototype measurements [3]. This leads to extended development periods and increased costs for the material. The solution to this challenge is the utilization of the numerical simulation that can precisely capture the mechanical behavior of the composite during the preforming process [4].

To obtain the well-defined constitutive model and the simulation schemes for the numerical calculation, characterization of the material is necessary [5]. Several experimental methods to characterize the material are proposed here: the uniaxial tension tests are used to characterize the tensile modulus along the fiber yarns; the bias-extension tests are used to characterize the shear modulus of the prepreg; the friction tests are used to characterize the prepreg-prepreg and prepreg-tool interaction during the preforming process; and the bending tests are employed to characterize the bending stiffness along the yarns. The details for all four of these experimental methods is described in the following parts of this paper.

## UNIAXIAL TENSION TESTS

Uniaxial tension tests are used to obtain the tensile modulus along the fiber yarns during the preforming process. The experiment setting is shown below (see Figure 1) with the use of the Sintech 20/G tensile machine. The mechanical properties of the uncured epoxy in the prepreg is sensitive to temperature, so that the Instron 3111 temperature chamber was used here. Moreover, the digital image correlation (DIC) system VIC-3DTM Measurement System was utilized in this experiment to measure the strain distribution in samples.

In the uniaxial tension tests of the prepreg, the tensile modulus was determined from the fabric tensile test, not a yarn test, so that the tensile specimen could include as many unit cells as possible [5]. Tests at 23 °C, 50 °C and 80 °C were performed. To avoid slippage between the specimen and the clamps caused by the viscous epoxy, the two ends of the specimen were cured before the tests to harden the material and ensure the clamping force during the tests.

To compensate the size difference of the specimens, the engineering stress and strain are used to normalize the load and displacement data. The curves at different temperature are demonstrated below (see Figure 2). It can be seen that as the temperature increases, the undulation stage of the material becomes longer, and the tensile modulus during the settle-down region slightly reduces. This is reasonable considering the softening of the epoxy at high temperature. Because of this phenomenon, the strain and the stress at the end of the undulation stage, and the stiffness after the undulation stage were selected to properly describe the temperature effect on the uniaxial behavior of the prepreg.

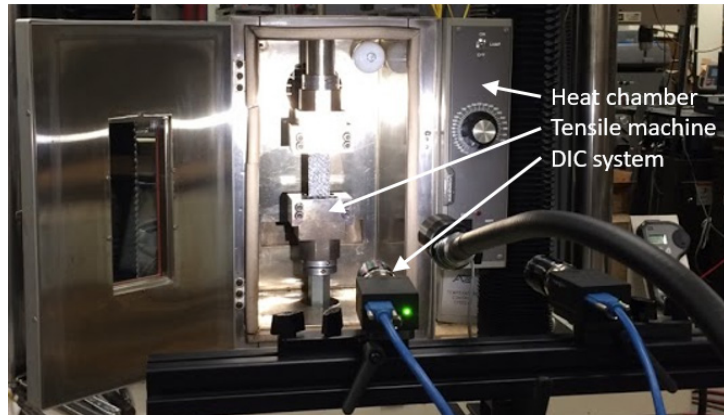


Figure 1. The experiment setting for the uniaxial tension and bias-extension tests.

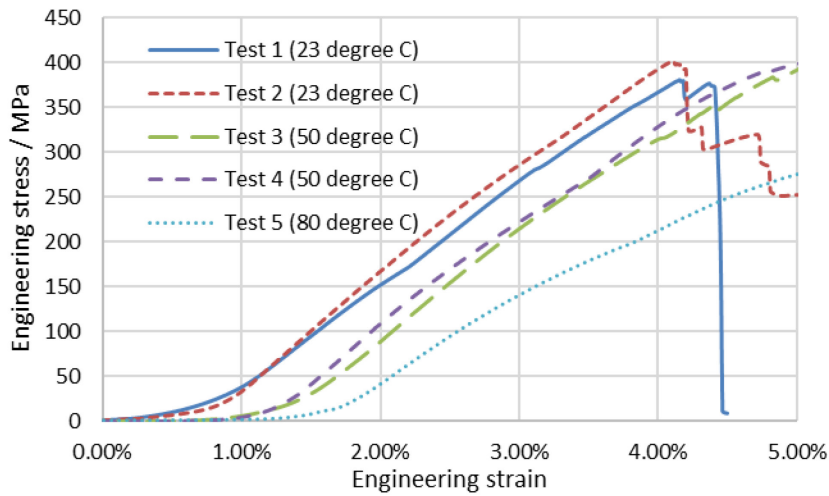


Figure 2. Engineering strain-stress curves from the uniaxial tension tests.

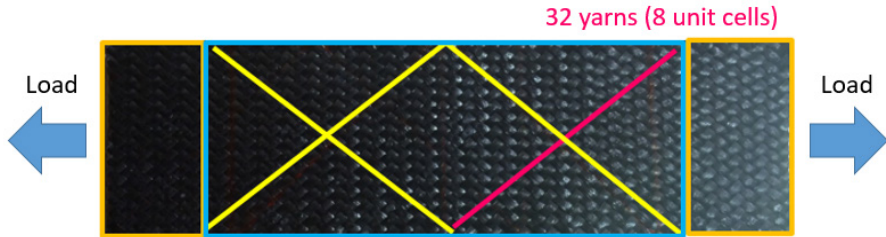


Figure 3. Specimen for the bias-extension tests.

## BIAS-EXTENSION TESTS

The bias-extension testing is a rather simple and accurate way, compared to other test methods, to determine the in-plane shear stiffness properties of the woven carbon fiber prepreg [6]. The experiment setting is the same as that for the uniaxial tension test (see Figure 1). To produce a pure shear central region, the fiber yarns were aligned  $\pm 45^\circ$  off the loading direction, and the length of the specimen should be larger than twice the width in order to release the constraint along the yarn direction (see Figure 3). There are

32 yarns in the specimen along each fiber yarn direction, resulting in 16 fiber yarns (4 unit cells) on each side of the central region.

The temperature of the experiment was set as 40 °C, 50 °C, and 60 °C, which covers the range of the general preforming process temperature measured by the IR camera during the single dome preforming process performed in our lab. All the tests were performed with the tensile rate of 12 mm/min. For the 60 °C tests, a different rate of 6 mm/min, was also included to investigate the effect of the shear rate on the shear stress. Under each condition set, the tests were performed 3-4 times and the results are averaged to reduce the test error.

Some normalization methods are necessary for convenient utilization of the load-displacement data from the bias-extension tests and compensation for the size difference of the specimen. The engineering stress was used to normalize the load. As for the displacement, because the deformation is not uniform throughout the specimen (see in Figure 4), the normalization method was derived as Eq. (1) based on the assumption that the yarns are inextensible and no slip occurs in the sample during the bias-extension tests [7].

$$u = \frac{d}{L-W} \quad (1)$$

where  $u$  is the normalized displacement,  $d$  is the crosshead displacement of the tensile machine,  $L$  is the initial length of the specimen, and  $W$  is initial the width of the specimen.

In order to validate this displacement normalization method, two bias-extension tests with different specimen sizes were performed. The parameters for the tests are listed below (see Table 1). The tensile rates are selected so that the normalized tensile rates are the same for both tests. From the result (see Figure 5), it can be seen that this displacement normalization method can properly compensate for the specimen size difference before shear locking when the large pure shear deformation happens in the central region.

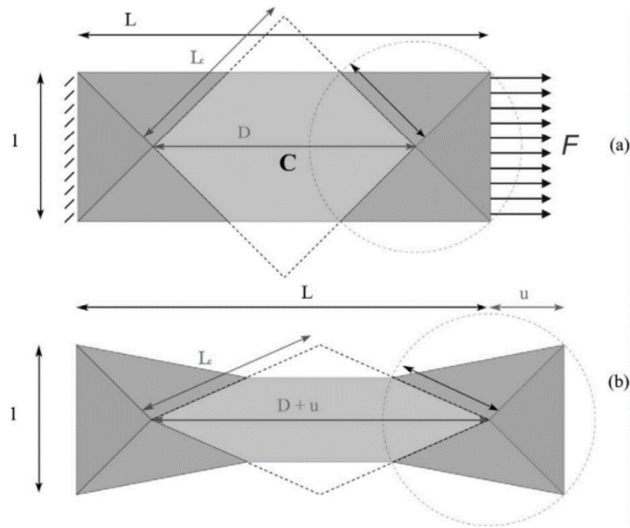


Figure 4. The bias-extension test specimen in (a) undeformed state and (b) deformed state [7].

TABLE I. PARAMETERS FOR THE DISPLACEMENT NORMALIZATION METHOD IN THE BIAS-EXTENSION TESTS.

Test	Size (width*thickness*length)	Tensile rate	Temperature
Short specimen	50 mm * 1.1 mm * 104.31 mm	12.00 mm/min	60 °C
Long specimen	51 mm * 1.1 mm * 136.00 mm	18.87 mm/min	60 °C

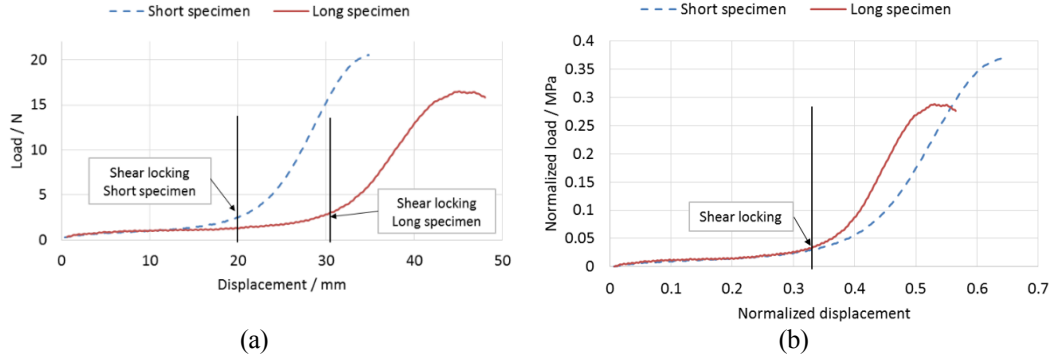


Figure 5. Bias-extension test results for different specimen sizes: (a) original load-displacement curves and (b) normalized load-displacement curves.

The normalized load-displacement curves under different experiment conditions are plotted (see Figure 6). It can be seen that the temperature plays an important role to the shear stress-strain relationship, especially at the temperature near 40 °C, which is the point where the used epoxy begins to transfer from the solid state to the fluid state. The higher the temperature, the lower the measured stress. The possible reason for this is that at a higher temperature, the epoxy becomes softer, reducing the resistance for the fiber warp and weft yarns to rotate relatively. As for the deformation-rate effect, a higher deformation rate will lead to a higher final stress, which is reasonable because the deformation resistance caused by the viscosity of the epoxy would be larger in a higher deformation rate case. However, it is interesting to note that when the deformation is smaller, the increase of the load happens earlier at a smaller deformation. This phenomenon cannot be explained simply by the elastic or viscous behavior of the material. It may be worth further investigating this in the future.

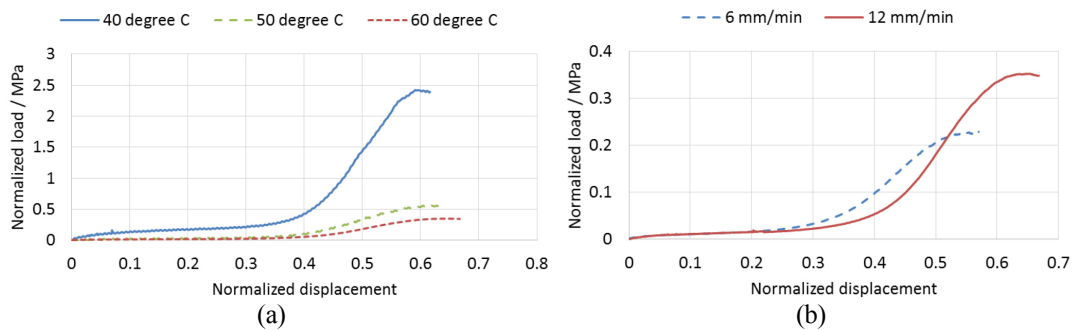


Figure 6. Bias-extension test results for (a) different temperatures and (b) different tensile rates.

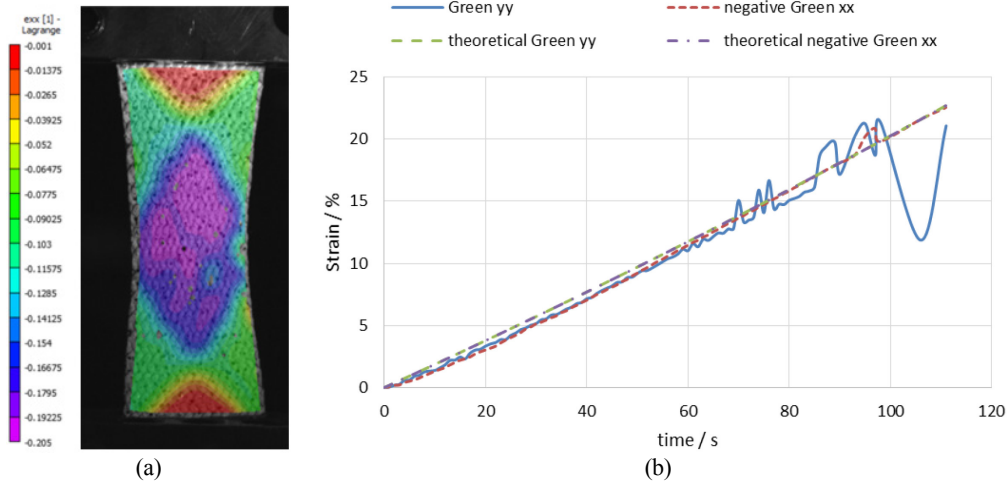


Figure 7. Validation for the kinematic assumption of the bias-extension tests from (a) Green strain field obtained from DIC and (b) average Green strain comparison in the central region.

In order to further validate the kinematical assumption that the yarns are inextensible and no slip occurs in the sample during the bias-extension tests [8], the digital image correlation (DIC) technique was applied to examine the Green strain field in the real specimen, and the result is compared with the theoretical one derived based on the same assumption (see Figure 7). It can be seen that in the range where the DIC can work properly, the assumption holds well. When the shear deformation becomes large, however, the relative motion between the warp and weft yarns would scratch off the paint used for detecting the strain in the DIC system and the result can no longer be reliable. Reference to the work of several other, there might be some slippage that occurs between the warp and weft yarns when the shear deformation was large [9]. Advanced optical methods might be necessary in future work in order to validate the assumption further and get a more precise relation between the shear deformation and stress, which can help examine the strain field of the prepreg under large shear deformation during the bias-extension tests.

## FRICTION TESTS

In the preforming process and when the woven prepreg layers have different fiber orientations, there might be some relative motion during the deformation because of the anisotropic properties of the material and the wavy surface topography. Compared to the ideal slip-free preforming process, fiber slip should affect the fiber orientation after forming, and as a result, alter the mechanical behavior of the final part. For this reason, it is necessary to measure this surface interaction behavior between the prepreg layers precisely.

As mentioned previously, the preforming process was performed with a gradually decreased temperature, and the relative motion speed between the prepreg layers also varies with the location. Taking these two key points into consideration, the experiment facility (see Figure 8) for these interaction tests was built on a displacement-controlled platform to introduce a relative motion under a normal pressure. A heated stage was used to impose a controlled temperature.

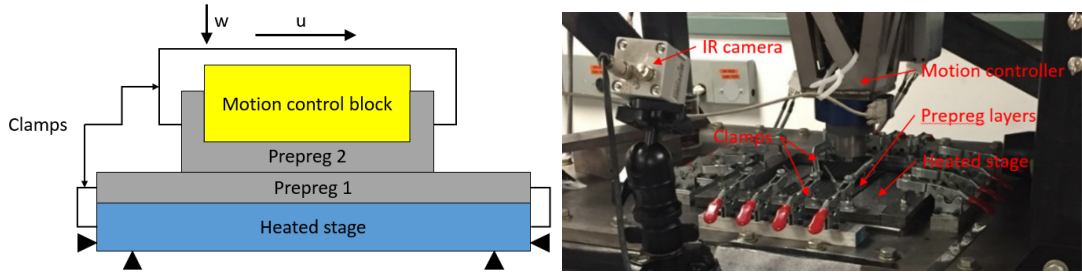


Figure 8. The experiment instrument for the composite prepreg friction test.

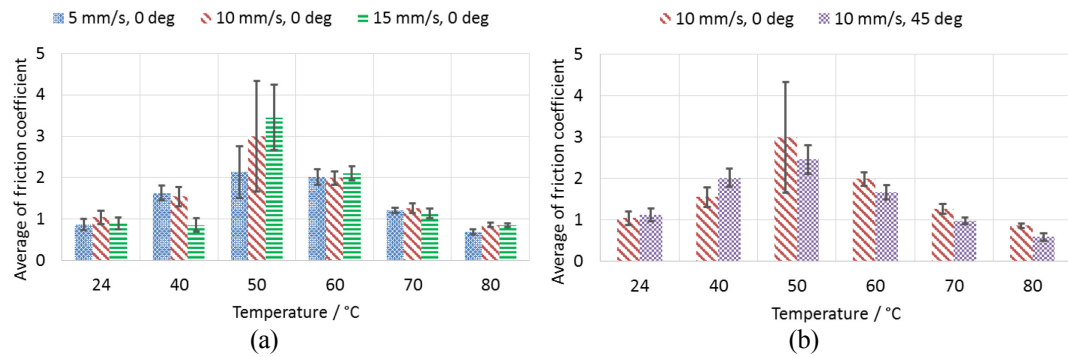


Figure 9. Temperature-friction coefficient bar column plots for (a) different relative motion speed and (b) different relative fiber orientation.

Before performing the tests, one layer of prepreg was clamped to the heated stage while the other one was clamped to the motion controlled block. The fiber orientations of these two layers were aligned parallel to each other. The prepreg on the top went through all the way to the side surfaces of the block in order to avoid breakage of the edges. To introduce the normal pressure, the block will first move down in the vertical direction. Because the heated stage and the block are not perfectly parallel, the normal pressure would fluctuate during the test (from 3.4 kPa to 14.2 kPa in the current setting). However, it was found that the friction coefficient did not change much in this pressure range; which follows the Coulomb law of kinetic friction. Hence, it was not necessary to do an accuracy control of the normal pressure. In order to investigate the effects of temperature and relative motion speed on the friction coefficient, the test speeds were selected as 5, 10, or 15 mm/s, and the temperature was set at 24 (room temperature), 40, 50, 60, 70, or 80 °C. A set of tests of two prepreg layers that have 45° fiber orientation difference from each other and 10 mm/s motion speed were also performed to investigate the effect of the fiber alignment by comparison with the results obtained from the test above mentioned.

During the tests, both the vertical and horizontal forces were documented at the frequency of 250 Hz. The Coulomb friction coefficients, which are also used in our simulation model as an effective interaction parameter, were calculated for all data points in each test as the indicator for the strength of the interaction. Both the average and standard deviation values of the friction coefficient at all different test settings were calculated and plotted (see Figure 9).

The plots of Figure 9 reveal that both the average and standard deviation of the friction coefficient reach to the highest points at 50 °C, which is the temperature for the resin in the prepreg to transit from its solid state to the fluid state. From room temperature all the way up to about 50 °C, the prepreg is in solid state and softens with the increase of the temperature. The average and standard deviation values of the friction coefficient both increase because the resin in the prepreg becomes stickier. When the temperature rises beyond 50 °C, the resin finishes the transition to the viscous fluid state. As a result, the prepreg acts like a soft cloth with the lubrication from the fluid resin. At this state, further temperature rise reduces the viscosity, leading to the reduction of the friction coefficient.

The effect of relative motion speed is weak at the room temperature, where the prepreg is still solid, and it is not very strong either at temperatures higher than 60 °C, where the viscosity of the resin is low and does not contribute much to the interactions between the two prepreg layers. However, the friction coefficient has an obvious positive relation to the motion speed at 50 °C, at which the resin becomes very sticky and viscous. At this temperature a higher speed leads to a stronger interaction, resulting in a larger friction coefficient between the prepreg layers. The situation at 40 °C is different though, in that the friction decreases when the motion speed increases. This difference may be caused by test error, since the friction at 15 mm/s and 40 °C is not only smaller than the ones of 5 and 10 mm/s, but also smaller than the one at 24 °C. This change does not follow the trends of the result when the motion speed is 5 or 10 mm/s. More tests will be performed at this state to investigate the cause of this phenomenon.

As for the orientation effect, when the temperature is lower than 50 °C, the friction coefficient is larger when the top and bottom fiber yarns were aligned to the same direction (see Figure 9) because the fibers in different layers are more likely to stick with each other in this situation. This explanation is also true for the fact that there were generally larger variations in the friction coefficient when the fibers were in the same direction, especially at 50 °C when the sticky resin made it more difficult for the stuck fibers to be separated from each other again. An opposite phenomenon was observed, however, when the temperature was low and the prepreg was in the solid state, where the ±45° orientation leads to higher friction (see Figure 9). This phenomenon requires further theoretical analysis for an in-depth understanding of the solid state prepreg interaction.

The test results suggest that for the preforming process where the temperature should be kept sufficiently high to ensure the fluid-state resin, the interaction between the prepreg layers is largely determined by the local temperature. The fiber orientation and relative motion speed only play minor roles here.

## BENDING TESTS

The bending stiffness of the material is also needed for proper simulation of the material behavior during the forming process. However, the softness of the prepreg under the preforming temperature makes it difficult to measure the bending stiffness via the standard 3-point bending test. An alternative bending stiffness test method was applied to measure the bending stiffness based on the tensile stiffness obtained in the uniaxial tension tests mentioned above.

The bending test method adopted in this work is similar to those proposed by Peirce et al. [10] and Lisa et al. [11]. In the experiment, one end of the rectangular prepreg sample was clamped horizontally on a support as a cantilever beam (see Figure 10). The prepreg would deform under gravity due to its low rigidity in the elevated temperature. The deflection of the sample tip was measured, and the deformed shape was analyzed by a digital image analysis. The entire system was placed in a temperature controlled chamber, and the temperature was recorded. The prepreg deformation during the test at 50 °C of the chamber temperature was given here as a demonstration (see Figure 10).

Note that in the experiment, the fiber was usually twisted due to the uneven clamping conditions. In order to minimize the error, the individual datum points were extracted along the central line in the image processing (see Figure 11). Given the size and the density of the prepreg material, the distributed load could also be calculated. However, due to the strong geometric nonlinearity, the bending stiffness could not be directly calculated from the typical beam theory. In this work, a simulation model was utilized to calculate the bending stiffness reversely. This simulation model utilized the homogeneous material properties. The compressive modulus of the material was modified until the same end tip displacement as the experimental result was reached. Then the effective compression stiffness could be obtained to properly describe the bending behavior of the prepreg. For example, at 50 °C, the tensile modulus of the prepreg is 9.34 GPa and the undulation of the specimen during the bending test is 1.5%, the reverse calculations in the simulation rendered the compressive stiffness of 14 MPa. The final prepreg curve from the simulation is also plotted in Figure 11 for comparison.

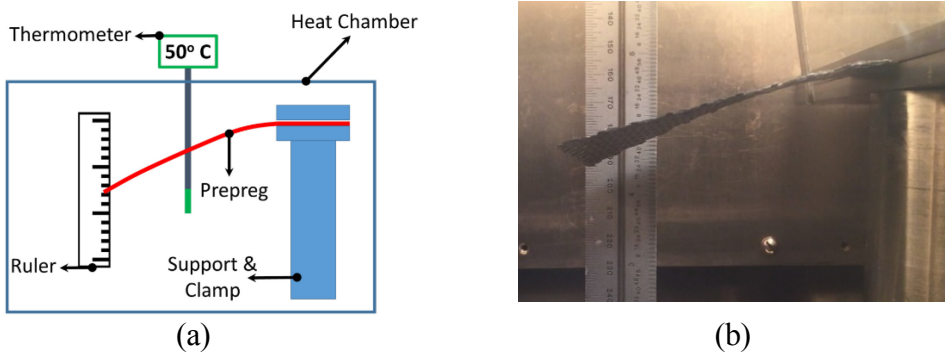


Figure 10. (a) Schematic of the bending test setup and (b) the shape of prepreg at 50 °C.

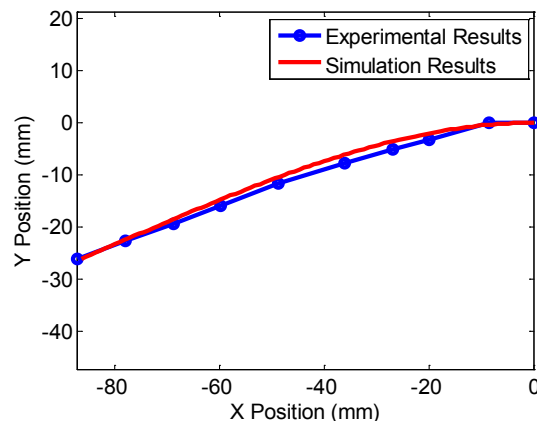


Figure 11. Digitalized prepreg curve from the 50 °C experiment and that from the reverse calculation.

## CONCLUSIONS AND FUTURE WORK

Characterizations of the tensile, and compressive, shear and frictional properties of the uncured woven prepreg are reported. All these tests were conducted in the temperature range appropriate for the material process. In the uniaxial tension tests, the strain-stress pair at the end of the undulation stage and the tensile stiffness after the undulation are selected to characterize the tensile behavior along the fibers. The prepreg was cured at the ends to ensure the clamping force under high loading state. In the bias-extension tests, a normalization algorithm of the crosshead displacement, based on the fiber inextension and no-slipage kinematical assumption, was proposed and validated by experiments. In the friction tests, the surface interaction was characterized with respect to relative motion speed, temperature, and fiber orientation. In the bending tests, the small bending stiffness was obtained via reverse calculation based on the comparison of the bending shapes from the measurement utilizing the gravity of the material and the simulation with the same configuration.

In order to further refine the test procedures and complete the input parameters necessary for the proposed modeling, the following work should be conducted in the near future: (1) a more advanced optical technique may be applied to validate the no-slipage and no-extension assumptions in the bias-extension tests, which can also help obtain more accurate shear deformation measurement when the shear angle is large; (2), a theoretical analysis on the surface interaction at the temperature ranging from 40 to 50 °C is necessary for in-depth understanding of the friction test results, especially for the effect of the viscous and sticky resin between the prepreg layers during the preforming process; and (3) the clamp design should be improved to avoid fiber twist, and the influence of fiber direction should also be included.

## ACKNOWLEDGEMENT

This work was supported by a subcontract from the Ford Motor Company with funding from the Office of Energy Efficiency and Renewable Energy (EERE), U.S. Department of Energy, under Award Number DE-EE0006867.

## REFERENCES

1. Che D, Saxena I, Han P, Guo P, Ehmann KF. Machining of carbon fiber reinforced plastics/polymers: A literature review. *Journal of Manufacturing Science and Engineering*. 2014 Jun 1;136(3):034001.
2. Jauffrè D, Sherwood JA, Morris CD, Chen J. Discrete mesoscopic modeling for the simulation of woven-fabric reinforcement forming. *International Journal of Material Forming*. 2010 Sep 1;3(2):1205-16.
3. Ten Thije RH, Akkerman R, Huétink J. Large deformation simulation of anisotropic material using an updated Lagrangian finite element method. *Computer methods in applied mechanics and engineering*. 2007 Jul 1;196(33):3141-50.
4. Hamila N, Boisse P, Sabourin F, Brunet M. A semi-discrete shell finite element for textile composite reinforcement forming simulation. *International journal for numerical methods in engineering*. 2009 Sep 17;79(12):1443-66.

5. Lee W, Um MK, Byun JH, Boisse P, Cao J. Numerical study on thermo-stamping of woven fabric composites based on double-dome stretch forming. *International journal of material forming*. 2010 Sep 1;3(2):1217-27.
6. Boisse P, Hamila N, Guzman-Maldonado E, Madeo A, Hivet G, Dell'Isola F. The bias-extension test for the analysis of in-plane shear properties of textile composite reinforcements and prepgs: a review. *International Journal of Material Forming*. 2016:1-20.
7. Wang P, Hamila N, Pineau P, Boisse P. Thermomechanical analysis of thermoplastic composite prepgs using bias-extension test. *Journal of Thermoplastic Composite Materials*. 2012 Aug 9:0892705712454289.
8. Cao J, Akkerman R, Boisse P, Chen J, Cheng HS, De Graaf EF, Gorczyca JL, Harrison P, Hivet G, Launay J, Lee W. Characterization of mechanical behavior of woven fabrics: experimental methods and benchmark results. *Composites Part A: Applied Science and Manufacturing*. 2008 Jun 30;39(6):1037-53.
9. Wang J, Page JR, Paton R. Experimental investigation of the draping properties of reinforcement fabrics. *Composites Science and Technology*. 1998 Dec 31;58(2):229-37.
10. Peirce FT. 26—The “handle” of cloth as a measurable quantity. *Journal of the Textile Institute Transactions*. 1930 Jan 1;21(9):T377-416.
11. Dangora LM, Mitchell CJ, Sherwood JA. Predictive model for the detection of out-of-plane defects formed during textile-composite manufacture. *Composites Part A: Applied Science and Manufacturing*. 2015 Nov 30;78:102-12.